CHISEL D.2019.4.2.2 – CU ALLOY – LATE BRONZE AGE – FRANCE

Artefact name   Chisel D.2019.4.2.2

Authors   Christian. Degrigny (HE-Arc CR, Neuchâtel, Neuchâtel, Switzerland) & Naima. Gutknecht (HE-Arc CR, Neuchâtel, Neuchâtel, Switzerland) & Valentina. Valbi (Laboratoire Métallurgie et Culture LMC-IRAMAT-CNRS-UTBM, Belfort, Franche-Comté, France)

Url   /artefacts/1253/

⌄ The object

Fig. 1: Chisel covered with a brown crust and blue-green corrosion products and showing areas of flaking,
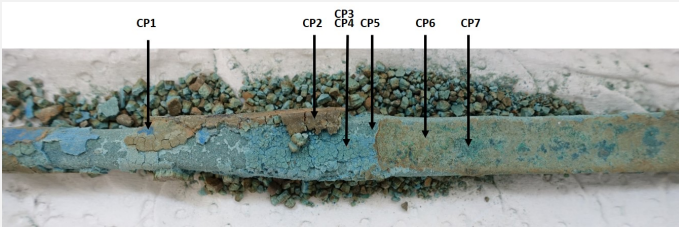
Credit HE-Arc CR, N.Gutknecht.

⌄ Description and visual observation

|	
Description of the artefact	Pointed elongated tool used for piercing holes. It is covered with brown crust and blue-green corrosion products that show areas of flaking. Dimensions: L = ca. 13cm. W = ca. 3cm.
Type of artefact	Tool
Origin	Granges Feuillet, dépôt n°2, Salins-les-Bains, Franche-Comté, France
Recovering date	2012
Chronology category	Late Bronze Age
chronology tpq	1350 B.C. ⌄
chronology taq	1150 B.C. ⌄
Chronology comment	
Burial conditions / environment	Soil
Artefact location	Musée de Lons-le-Saunier, Lons-le-Saunier, Franche-Comté
Owner	Musée de Lons-le-Saunier (dépôt de Salins-les-Bains)
Inv. number	D.2019.4.2.2
Recorded conservation data	N/a

Complementary information

From the time of excavation in 2012 until its entry into the museum in 2015, the object was kept in a food storage box in an uncontrolled environment. Flaking corrosion was documented when the object was collected and stored by the museum in 2015.

⊻ Study area(s)

Credit HE-Arc CR, N.Gutknecht.

Fig. 2: Location of the different corrosion products. The codes are those of Fig. 4,
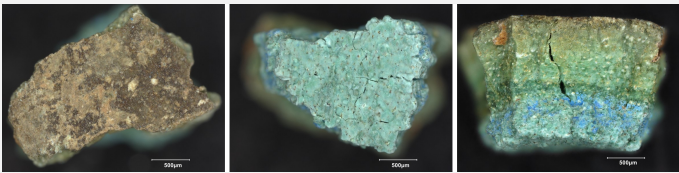

Credit LMC-CNRS, V.Valbi.

Fig. 3: Fragment of the entire corrosion structure detached from the object and collected for analysis. Appearance of the external (left), internal (middle) and side view (right) surfaces,

⊻ Binocular observation and representation of the corrosion structure

The schematic representation below gives an overview of the corrosion structure encountered on the chisel from a first visual macroscopic observation.

Strata	Type of stratum	Principal characteristics
CP1	Corrosion product	dark blue, thin, scattered, compact, brittle, soft
CP2	Corrosion product	light brown, medium, discontinuous, compact, very hard
CP3	Corrosion product	green, thick, discontinous, non-compact, very soft
CP4	Corrosion product	blue, thin, discontinuous, non-compact, soft
CP5	Corrosion product	dark green, medium, continuous, non-compact, very soft
CP6	Corrosion product	light orange, thin, isolated, non-compact, very soft
CP7	Corrosion product	dark green, thin, isolated, compact, soft

Table 1: Description of the principal characteristics of the strata as observed under binocular and described according to Bertholon's method.
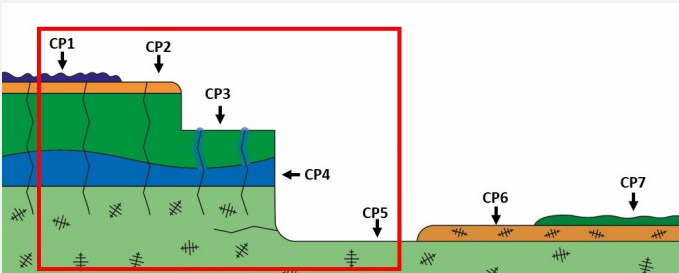
Credit HE-Arc CR, N.Gutknecht.

Fig. 4: Stratigraphic representation of the corrosion structure of the chisel by macroscopic and binocular observation with indication of the corrosion structure used to build the MiCorr stratigraphy of Fig. 5 (red square),
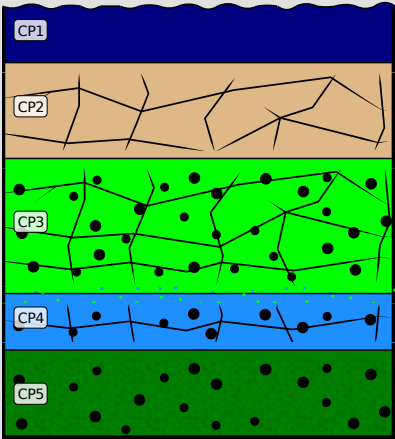
Fig. 5: Stratigraphic representation of the chisel observed macroscopically under binocular using the MiCorr application with reference to Fig. 4. The characteristics of the strata are only accessible by clicking on the drawing that redirects you to the search tool by stratigraphy representation, Credit HE-Arc CR, N.Gutknecht.
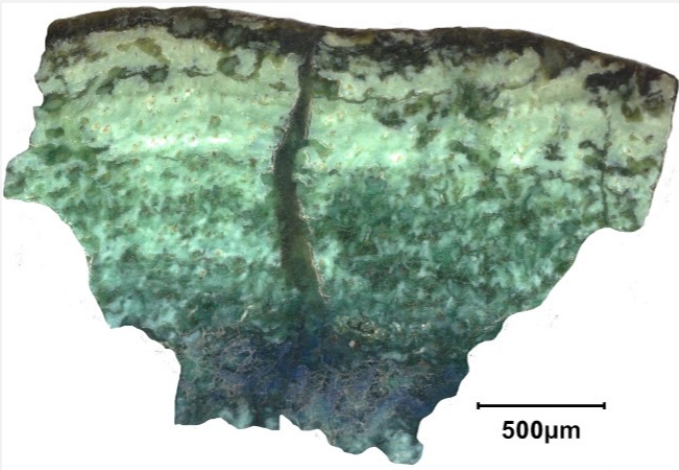
≫ Sample(s)

Fig. 6: Micrograph of the cross-section of a fragment detached from the chisel in dark field,

Credit LMC-CNRS, V.Valbi.

Description of sample	A fragment was selected from those corrosion products that spontaneously detached from the object.
Alloy	Cu Alloy
Technology	Cast
Lab number of sample	
Sample location	Centre de Conservation et d'Etude René-Rémond, Lons-le-Saunier
Responsible institution	Centre de Conservation et d'Etude René-Rémond, Lons-le-Saunier
Date and aim of sampling	April 2021

Complementary information

None.

Invasive approach (on the sample)

- Optical microscopy: the sample is polished, then it is observed with a numerical microscope KEYENCE VHX-7000 in bright and dark field.

- SEM-EDX: the sample is coated with a carbon layer, then analyses are performed on a SEM-FEG JEOL 7001-F equipped with a silicon-drift EDX Oxford detector (Aztec analysis software) with an accelerating voltage of 20 kV and probe current at about 9 nA. The relative error is considered of about 10% for content range <1mass%, and of 2% for content range of >1mass%.

- μ-Raman spectroscopy: it is performed on a HORIBA Labram Xplora spectrometer equipped of a 532 nm laser with 1800 grating, the laser power employed is between 0.04 and 0.55 mW with acquisition time varying between 1 and 5 minutes.

⇓ Non invasive analysis

None.

⇓ Metal

As it was not possible to cut the object to collect samples, the metal could not be documented. Only external corrosion layers were analyzed.

Microstructure	None
First metal element	Cu
Other metal elements	Sn

Complementary information

None.

⇓ Corrosion layers

The observation of the sample in cross-section in dark field allowed to identify an external brown 200 μm thick stratum (CP1), a green 1000 μm thick stratum (CP2), a turquoise 400 μm thick stratum (CP3) with blue aggregates.

The EDX analysis of the identified strata shows that the whole corrosion structure is Cu depleted and Sn enriched and polluted with external elements such as Fe, Al, Si and P. This Sn-rich phase was analysed by Raman spectroscopy (R01) and shows a broad band at 560 cm^{-1} that can be attributed to nanocassiterite (SnO$_2$) by comparison to the work of Ospitali et al. 2012. A sharp peak at 999 cm^{-1} is also observed and could be attributed to the presence of phosphates.

S-rich dark inclusions (Figs. 8-9) were observed in the whole corrosion structure and were identified as covellite (CuS) by Raman spectroscopy (R04).

The blue aggregates in the CP3 are Cu enriched and were identified as azurite (Cu$_3$(CO$_3$)$_2$(OH)$_2$) by Raman spectropscopy (R10).

	CP1	CP2	CP3	CP3 aggregates
O	35	28	30	37
Sn	47	55	50	17
Cu	11	11	15	42
Si	1	1	1	<0.5
Al	2	1	<0.5	1
Fe	2	1	2	<0.5
P	<0.5	<0.5	1	<0.5

Table 2: Chemical composition (mass%) of the corrosion layers over a general area of analysis in cross-section obtained by SEM-EDX, LMC-IRAMAT-CNRS-UTBM.
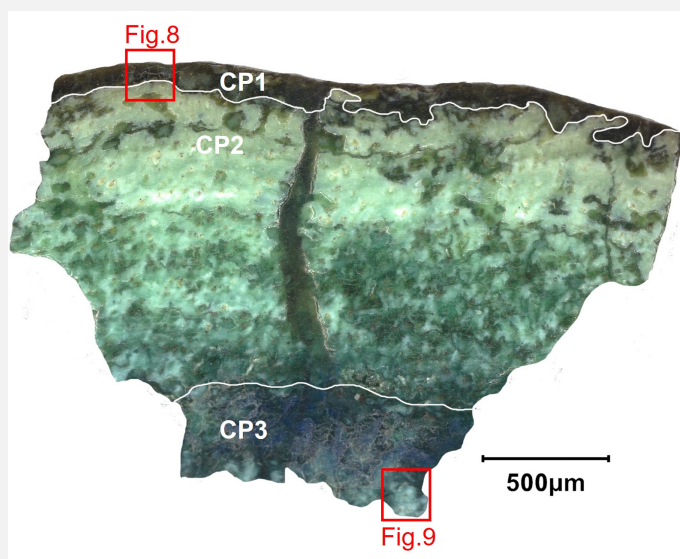

Credit LMC-CNRS, V.Valbi.

Fig. 7: Micrograph of the cross-section of the sample in dark field with the identification of the CPs,
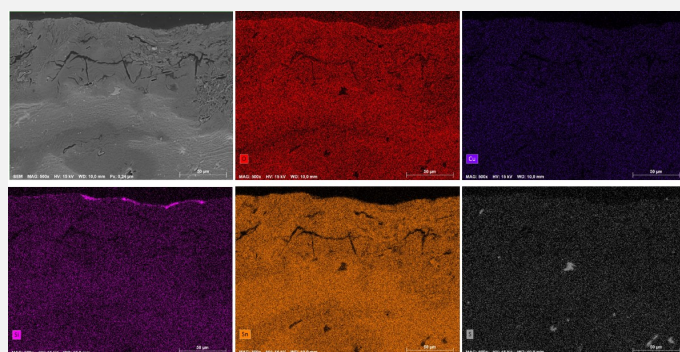

Credit

Fig. 8: SEM image, SE-mode, and elemental chemical distribution of the selected area,
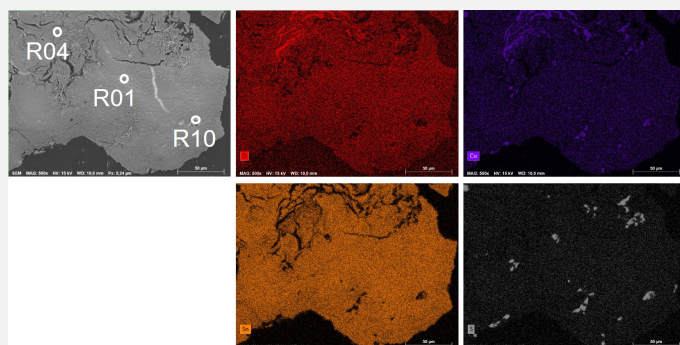

Credit LMC-CNRS, V.Valbi.

Fig. 9: SEM image, SE-mode, and elemental chemical distribution of the selected area. The selected points for Raman analysis shown in Fig. 10 are indicated,
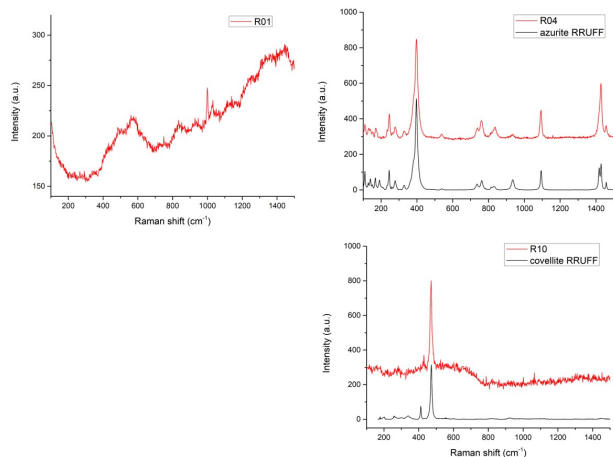
Corrosion form   Uniform

Corrosion type   Unknown

Complementary information

None.

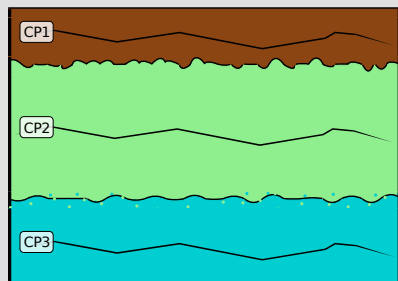## ⩔ MiCorr stratigraphy(ies) – CS

Fig. 10: Stratigraphic representation of the fragment of the chisel observed in cross-section under dark field using the MiCorr application. The characteristics of the strata are only accessible by clicking on the drawing that redirects you to the search tool by stratigraphy representation. This representation was build according to Fig. 7, Credit LMC-CNRS, V.Valbi.

⩔ Synthesis of the binocular / cross-section examination of the corrosion structure

The stratigraphies obtained by binocular and cross-section observation show several differences. The sample observed in cross-section is collected from the flaked material and is thus representing a different location than the binocular observation performed on the whole object (Fig. 2).

The flaked sample used for the cross-section observation includes the corrosion layers above the "flaking interface" located between CP4 and CP5 in binocular view. Thus the strata under the flaking interface did not get sampled. CP1 from the binocular view was not observed in the selected sample either.

Fig. 11: Stratigraphic representation side by side of binocular view and cross-section (dark field),

Binocular   Correspondence   Cross-section
Dark field
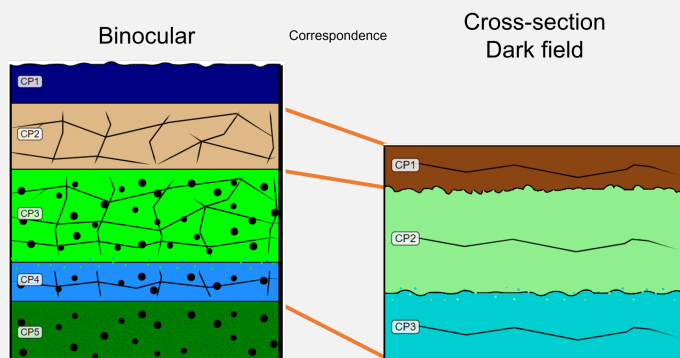
Credit HE-Arc CR, N.Gutknecht.

⌄ Conclusion

The corrosion structure has a homogeneous composition despite the colour differences observed. The fragment of the chisel from Salins-les-Bains shows an Sn enrichment typical of the decuprification phenomenon of bronze alloys. A local enrichment in copper is observed due to the formation of the hydroxycarbonate azurite in the most internal stratum. The dark covellite inclusions are most likely residuals of copper sulfide inclusions from the metal microstructure resulting from the smelting of S-containing ores.

⌄ References

References on analytical methods and interpretation

1. Lafuente, B., Downs, R. T., Yang, H., Stone, N. (2015) The power of databases: the RRUFF project. In: Highlights in Mineralogical Crystallography, T. Armbruster and R. M. Danisi, eds. Berlin, Germany, W. De Gruyter, 1-30.
2. Ospitali, F., Chiavari, C., Martini, C., Bernardi, E., Passarini, F., Robbiola, L. (2012) The characterization of Sn-based corrosion products in ancient bronzes: a Raman approach. Journal of Raman Spectrpscopy, 43 (11), 1596-1603.
3. Robbiola L., Blengino M., Fiaud C., (1998) Morphology and mechanisms of formation of natural patinas on archaeological Cu–Sn alloys. Corrosion Science, 40 (12), 2083-2111.